HHS Public Access

Author manuscript

Mol Cell. Author manuscript; available in PMC 2017 August 18.

Published in final edited form as:

Mol Cell. 2016 August 18; 63(4): 662–673. doi:10.1016/j.molcel.2016.06.020.

Essential roles for Polymerase θ mediated end-joining in repair of chromosome breaks

David W. Wyatt[1], **Wanjuan Feng**[1,2], **Michael P. Conlin**[1], **Matthew J. Yousefzadeh**[3], **Steven A. Roberts**[4], **Piotr Mieczkowski**[5], **Richard D. Wood**[3], **Gaorav P. Gupta**[1,2], and **Dale A. Ramsden**[1]

[1]Lineberger Comprehensive Cancer Center, Curriculum in Genetics and Molecular Biology, and Department of Biochemistry and Biophysics, University of North Carolina at Chapel Hill, Chapel Hill, North Carolina 27599, USA

[2]Department of Radiation Oncology, University of North Carolina at Chapel Hill, Chapel Hill, North Carolina 27599, USA

[3]Department of Epigenetics and Molecular Carcinogenesis, University of Texas MD Anderson Cancer Center, Smithville Texas 78597, USA

[4]School of Molecular Biosciences, Washington State University, Pullman, Washington 99164, USA

[5]Department of Genetics, University of North Carolina, Chapel Hill, North Carolina 27599 USA

Summary

DNA Polymerase theta (Pol θ) mediated end-joining (TMEJ) has been implicated in repair of chromosome breaks, but its cellular mechanism and role relative to canonical repair pathways is poorly understood. We show it accounts for most repair associated with microhomologies, and is made efficient by coupling a microhomology search to removal of nonhomologous tails and microhomology-primed synthesis across broken ends. In contrast to nonhomologous end-joining (NHEJ), TMEJ efficiently repairs end structures expected after aborted homology-directed repair (5′ to 3′ resected ends) or replication fork collapse. It typically does not compete with canonical repair pathways, but in NHEJ-deficient cells is engaged more frequently and protects against translocation. Cell viability is also severely impaired upon combined deficiency in Pol θ and a factor that antagonizes end resection (Ku or 53BP1). TMEJ thus helps sustain cell viability and genome stability by rescuing chromosome break repair when resection is misregulated or NHEJ is compromised.

Correspondence: dale_ramsden@med.unc.edu.

Author Contributions: D.A.R., G.P.G, R.D.W, and D.W.W. designed the studies and analyzed the data. D.W.W. and M.J.Y. generated and characterized cell lines deficient in Pol θ and Ku70 and variants. D.W.W. performed end-joining, translocation, and cell proliferation assays. W.F. performed immunofluorescence and colony formation assays. M.P.C. performed homologous recombination assays. D.W.W. and S.A.R. performed bioinformatic analyses. D.A.R. and D.W.W. wrote the manuscript with input from all authors.

eTOC Blurb

Wyatt et al show Polymerase θ accounts for most microhomology-dependent chromosome break repair, and outline a mechanism that makes this pathway efficient and flexible. They define biologically relevant substrates, determine it is essential in cells that inappropriately regulate resection, and that it can both positively and negatively impact genome stability.

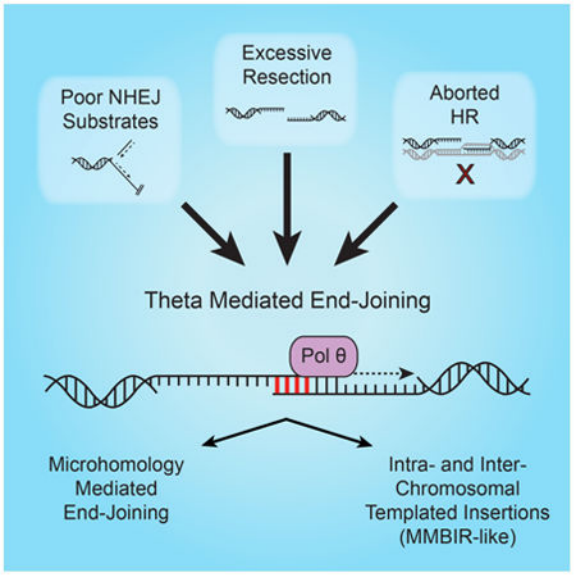

Introduction

Repair of chromosome double strand breaks (DSBs) is essential for normal cell growth and resistance to exogenous break-inducing agents. At the organismal level DSB repair also protects against cancer, shapes the response to cancer therapy, and has specialized roles in germ cell and immune system development. Mammalian cells typically rely on two pathways for DSB repair: classically defined non-homologous end-joining (NHEJ) and homologous recombination (HR). Resection, the excision of 5′ terminal strands of the broken ends to expose long 3′ ssDNA tails, is an essential intermediate in HR and helps channel DSBs to repair by this pathway (Aparicio et al., 2014).

A third DSB repair pathway, termed Alternative NHEJ or microhomology-mediated end-joining (Alt-NHEJ/MMEJ), has also been described. Alt-NHEJ was initially defined as both independent of factors required for NHEJ and associated with deletions clustered at 3 to 6 base pair (bp) sequence identities (“microhomologies”) in flanking DNA (Boulton and Jackson, 1996; Kabotyanski et al., 1998). Such products also typically require factors that promote resection (e.g. CtIP and Mre11) (Sfeir and Symington, 2015) indicating that, like HR, Alt-NHEJ typically acts downstream of this step.

Alt-NHEJ/MMEJ in metazoans has also been linked to activity of DNA polymerase theta (Pol θ; encoded by *Polq*) (Chan et al., 2010; Roerink et al., 2014; Yousefzadeh et al., 2014). By comparison, an ortholog for metazoan Pol θ is missing in yeast (Sfeir and Symington, 2015), where synthesis during MMEJ has instead been associated with the combined activity

of multiple polymerases (Lee and Lee, 2007). Pol θ is a 290kDa protein with a super family 2 helicase-like domain in the N-terminal third, and a Family A DNA polymerase domain in the C-terminal third (Yousefzadeh and Wood, 2013). Both *in vitro* and cellular experiments indicate it promotes MMEJ by using one 3′ ssDNA overhang as a synthesis primer, after annealing this overhang to a second ssDNA overhang at a short tract of complementary sequence (Kent et al., 2015; Yousefzadeh et al., 2014). Strikingly, Pol θ is frequently over-expressed in HR-deficient cancers and overexpression is linked to poor prognosis (Ceccaldi et al., 2015; Higgins et al., 2010; Lemée et al., 2010). Pol θ can also be essential in the context of HR deficient cancer cell lines (Ceccaldi et al., 2015; Mateos-Gomez et al., 2015), identifying it as a promising therapeutic target.

The mechanistic constraints on Pol θ activity in cellular repair and the relationship between this pathway and canonical DSB repair pathways (NHEJ, HR) are still unclear. We investigated these questions through use of extra-chromosomal and chromosomal assays and a panel of mouse embryo fibroblast lines (MEF) cell lines deficient in *Polq*, NHEJ (*Ku70*), and factors implicated in control of end resection and repair pathway choice (*Mre11, 53BP1*). Our results provide insight into how Pol θ activity contributes to cellular DSB repair. We show Pol θ activity is facilitated by an ability to couple microhomology primed synthesis to a “microhomology search” and removal of non-homologous tails. We further identify an essential role for this enzyme in rescuing repair of DSBs in contexts where the ability to appropriately regulate end-resection has been compromised.

Results

Distinct substrates for NHEJ and Pol θ mediated end-joining

We previously showed that Pol θ is required for a cellular end-joining pathway – Polymerase θ mediated end-joining, or TMEJ – that is independent of Ku, and uniquely able to join ends with extended 3′ssDNA tails (Yousefzadeh et al., 2014). To better address the relationship between TMEJ and classically defined NHEJ we sought to make cell lines deficient in one or the other pathway, or both. We consequently employed CRISPR/Cas9 to generate variants of existing isogenic wild type and *Polq*$^{-/-}$ MEF lines (Yousefzadeh et al., 2014)(Fig. S1A) that do not express significant Ku70 protein (Fig. S1B). These lines are deficient in NHEJ, and can be complemented by expression of introduced Ku70 cDNA (Fig. S1C). Importantly, bi-allelic mutation of the *Ku70* gene in *Polq*$^{-/-}$ cells was rare, and relative to the other cell types the isolated *Polq*$^{-/-}$*Ku70*$^{-/-}$ cell line had both low colony forming efficiency and a severe proliferative defect, (Fig. 1A). Combined loss of Ku70 and Pol θ is also associated with a reduced fraction of cells in S phase and increased chromosome aberrations (Fig. S1D, E). Expression of a Ku70 cDNA in this line was sufficient to correct the growth defect, confirming it could be attributed to combined loss of Ku70 and Pol θ. To further address this issue we performed a reciprocal experiment, by mutagenizing Pol θ in the context of cells already deficient in *Ku70*. Lentiviral infection of *Ku70* deficient cells with 3 different constructs that target mutations to the *Polq* gene, but not 3 different control target sites, severely reduced both the frequency and size of colonies formed (Fig. 1B). No significant differences in colony forming ability were observed when the same 6 viruses were introduced into wild type cells (Fig. S1F). Deficiencies in Ku70 and Pol θ thus have

synergistic effects on cell growth and viability - the doubly deficient cells are “synthetic sick”.

The progressive 5′ to 3′ resection of DSB termini is a necessary pre-requisite for repair of DSBs by homologous recombination (HR). To address how resection affects the deployment of different end-joining pathways we introduced a panel of linear double stranded DNA substrates with “pre-resected” ends, where 3′ ssDNA overhangs ranged from 4-70 nucleotides (nt) (Fig. 2A, S2A), into the cell lines described above. Head and tail overhang sequence were designed such that the terminal 4 nt were complementary, i.e. contain a microhomology. The impact of differing location and length of microhomologies is discussed in greater detail below.

Overall joining efficiency was reduced 5-10 fold for overhang lengths in excess of 10 nucleotides, and two populations of end-joining products were readily evident; one where most of both overhangs had been removed, and another where most of both overhangs had been retained (Fig. 2B-D). As overhang length is increased, joining is progressively more reliant on products where most of both overhangs are retained (Fig.S2A, S2B). In all contexts joining after overhang loss was largely dependent on Ku70/NHEJ, while joining associated with retention of 3′ overhangs was dependent on Pol θ (bottom panels, Fig. 2B-D). Pol θ additionally was not required for either product class (overhangs retained and overhangs lost) using a substrate where the overhang polarity was reversed (5′ overhang), but which was otherwise equivalent (Fig. S2C). TMEJ is thus uniquely employed for repair of products of 5′>3′ resection.

When the 3′ overhang was only 45 nt, overall joining efficiency was reduced 3-fold in Ku70 deficient cells and not affected by Pol θ deficiency (Fig. 2B, top panel). In contrast, the reciprocal pattern was observed when overhang length was increased to 70 nt (Fig. 2C, top panel). Only trace levels of end-joining were observed for both substrate variants in cells deficient in both Pol θ and Ku70 (Fig. 2B, 2C, top panels). The two pathways thus together account for most of the cellular capacity to repair pre-resected end structures, but TMEJ assumes prominence as the extent of 5′>3′ resection exceeds 45 nt (see also Fig. S2B).

We reasoned that this increased reliance on Pol θ-dependent repair as the ssDNA tails are extended reflects a reduced ability of the Ku heterodimer to load on substrates with long ssDNA tails (Fig. S2D). To further investigate this possibility, we generated a variant of the shorter 45 nt 3′ overhang with a “Y” or forked end structure, by including a 5′ streptavidin-blocked flap (Fig. 2D). Such a substrate is expected to completely block loading of Ku, and is analogous to products of replication fork collapse (“one ended breaks”). Accordingly, we observed no significant impact of Ku-dependent NHEJ when using this substrate. Repair was instead Pol θ-dependent (Fig. 2D, top panel) and consisted almost entirely of products that retained the majority of both 3′ overhangs (Fig. 2D, bottom panel), thus can be readily defined as TMEJ. We conclude Pol θ-dependent repair is most important when considering end structures where loading of Ku is impaired. This includes those end structures expected after aborted HR – ends with extended 3′ ssDNA tails - or after replication fork collapse.

Mechanism of Pol θ-mediated end-joining—Products that retain significant amounts of overhang are mostly dependent on Pol θ; conversely, Pol θ deficiency had little impact on either the efficiency or structure of those products generated after overhang loss (Fig. 2). Relocation of qPCR primers to require that end joining products retain at least 10 nt of each overhang is thus sufficient to restrict analysis to Pol θ-mediated events (Yousefzadeh et al., 2014)(Fig. 3A).

Pol θ is a multi-domain protein, with an N-terminal helicase-like domain and a C-terminal polymerase domain (Fig. S3A). To investigate the contributions of each activity we compared the ability to complement *Polq*$^{-/-}$ cells for TMEJ capacity by expression of the wild type *Polq* cDNA, a variant cDNA with a mutation inactivating ATPase activity of the helicase domain (K121M), or a variant cDNA with mutations that inactivate the polymerase domain (D2330A/Y2331A; Motif A) (Yousefzadeh et al., 2014). Levels of TMEJ in cells expressing the D2330A/Y2331A construct were indistinguishable from cells with an empty vector control (Fig. 3A); polymerase activity is thus essential for this pathway. In contrast, loss of ATPase activity in the helicase-like domain had no significant impact on joining efficiency, but did affect product spectra (discussed below). We also assessed a possible role for Pol μ and Pol λ, which have previously been associated with an ability to direct intermolecular DNA synthesis, i.e. can prime synthesis from a 3′ tail from one DSB end, and use a second DSB end as template (Pryor et al., 2015). Both of these polymerases are dispensable for cellular end-joining using pre-resected substrates (Fig. 3A), with levels of TMEJ instead increased in cells deficient in both Pol μ and Pol λ. This may reflect the important role of these polymerases in NHEJ, and increased TMEJ in NHEJ-deficient contexts.

The substrates described above were designed such that the terminal 4 nt were complementary, to allow for alignment-directed synthesis. Surprisingly, products consistent with synthesis from these terminal alignments accounted for only 56% of TMEJ when using the 45 nt 3′ overhang substrate, and 20% of TMEJ when using the 70 nt 3′ overhang substrate (Fig. 3B; Table S1). Remaining products favored alignments with short complementary sequences found internally (“embedded” alignments). For example, repair of the 70 nt overhang substrate frequently employed all four of the alignments that are greater than 3 bp and can also be found within 25 nt of the 3′ ends. Taken together, these 4 products account for 2/3rds of all products recovered (Fig. 3B), with the three embedded alignments used almost twice as often as the terminal alignment. Moreover, there were only mild effects on the efficiency of repair when using a substrate where both the terminal and most favored embedded alignments were disrupted (Fig. S3B). We additionally did not see significant recovery of products where an embedded alignment directed synthesis from a mispaired tail (Fig. 3B). We can therefore infer synthesis by Pol θ using embedded alignments is efficiently coupled to a prior step where the unpaired tail is removed.

Notably, the ability to use embedded alignments was modestly reduced in cells expressing the Pol θ variant with an ATPase inactivating mutation (K121M; Fig. 3C). This suggests TMEJ is facilitated by an active search for complementary sequence alignments (i.e. microhomology in finished product) that involves ATPase activity in the N-terminal helicase-like domain. Characterization of products also clarifies the constraints on this

putative microhomology search mechanism. Considering first the amount of complementary sequence, only those products with alignments > 2bp were significantly enriched (Fig. 3D). However, the length of nonhomologous tails impacts the ability to use such alignments. For example, a product generated from a 6 bp alignment, but which would generate long nonhomologous tails (52 nt and 22 nt), is observed 20-fold less frequently than a 4 bp alignment with short tails (9 nt and 2 nt, Fig. 3B). Alignments resulting in tails with one long and one short tail (e.g. 51 nt and 4nt, Fig. 3B) are also rarely used, suggesting a need to recognize both 3′ termini. In sum, 91% of products recovered using the 70 nucleotide overhang substrate (140 nt of ssDNA) have deletion less than 50 bp (Table S1).

TMEJ rescues chromosome break repair when canonical pathways are compromised

We next addressed the relationship between TMEJ and canonical pathways (NHEJ, HR) in repair of a chromosome break by introducing a DSB with the Cas9 nuclease targeted to the *Rosa26* locus in Chromosome 6 (Fig. 4A). We then determined the effect of Pol θ and Ku70 deficiencies on repair of this break by end-joining (Fig.4, 5) and HR (Fig. 6), as well as the extent to which it is prone to participating in translocations with another Cas9-induced break (Fig. 6). We confirmed all cell types expressed comparable amounts of Cas9 (Fig. S4A), and assessed end-joining by sequencing the region flanking the target site. As it is not possible to distinguish uncut chromosome from error free repair, we consider as definitive products of end-joining only those sequences with insertions or deletions at the target site.

The majority (75%) of products in wild type (WT) cells had short 1-5 bp deletions, and deficiency in Pol θ had little impact on either the frequency or character of these products (Fig. 4B, S4B). This is consistent with a predominant role for NHEJ in repairing these breaks. By comparison, deletions that were both intermediate in size (between 5 and 50 bp) and associated with microhomologies were depleted in Pol θ deficient cells (reduced 4 fold; Fig. 4C). Expression of a WT *Polq* cDNA was sufficient to reverse this defect (Fig. S4C), and the effect of Pol θ on microhomology associated deletion was apparent for all microhomology lengths greater than 2 bp (Fig. S4D).

Deficiency in Ku70/NHEJ resulted in deletions that were both much larger and more frequently associated with microhomology (Fig. 4B, 4C). These microhomology-associated deletions were again mostly dependent on Pol θ (reduced 7 fold in $Polq^{-/-}Ku70^{-/-}$ cells), but the effect of Pol θ was no longer limited to the subset of deletions ranging from 5-50 bp (Fig. 4C). We additionally confirmed expression of a Ku70 cDNA in both Ku70 deficient cells ($Ku70^{-/-}$, $Polq^{-/-}Ku70^{-/-}$) was sufficient to return the frequency and pattern of microhomology associated deletions to that observed in the matched $Ku70^{+/+}$ parent cell lines (Fig. S4C). Comparison of end-joining spectra over time also indicates that TMEJ is engaged much more rapidly in Ku deficient cells (Fig. S4E). Therefore, relative to an NHEJ proficient background, TMEJ in Ku70 deficient cells accounts for a much larger fraction of repair, is engaged faster, and its influence now extends to large deletions.

Two classes of insertions had conspicuously distinct genetic requirements. Most insertions were short (1-4 bp) and generated during repair by NHEJ (reduced 7 fold in $Ku70^{-/-}$ cells; Table S2). In contrast, deficiency in Ku70 alone had the opposite effect on longer insertions (3 fold increase), and these longer insertions were dependent on Pol θ (Fig. 4D). To assess if

these Pol θ-dependent insertions were templated, we focused on the subset of insertions that were sufficiently large (>24 bp) to allow mapping to the mouse genome. Most of these insertions – 87% of those observed in *Ku70*$^{-/-}$ cells – could be mapped (i.e. were definitively templated) to sequence near the Cas9 target site in chromosome 6 (Table S2). A surprisingly high frequency (1.5×10^{-3} in *Ku70*$^{-/-}$ cells) of end-joining products recovered had insertions that used template from other chromosomes (Table S2), and were derived from both genic and intergenic regions. Template switching events, both intra- and inter-chromosomal, were often complex (Fig. 4E), with successive segments derived from template tracts separated by 100s of base pairs, and 2-3 bp microhomologies often evident in the flanks of successive segments. In some cases successive segments were derived from nearby DNA but employed the opposite strand as template. Insertions mediated by Pol θ are thus largely template-dependent, and provide striking evidence of the ability of this polymerase to promiscuously switch template.

We show above that in Ku deficient cells TMEJ/Pol θ is both engaged more rapidly and accounts for a much greater fraction of repair. Since extrachromosomal experiments indicated Pol θ acts only on pre-resected ends, we reasoned the synthetic effects of Pol θ and Ku deficiency on proliferative capacity could reflect excessive end resection associated with Ku70 deficiency, and a central role for TMEJ in rescuing repair of these ends. In accord with this model, mutagenesis of the *Mre11* gene, a factor implicated in end resection, had an impact on large deletion in *Ku70*$^{-/-}$ cells comparable to loss of Pol θ (Fig. 5A). This model also predicts there should be a genetic interaction between *Polq* and *53BP1*, a factor that promotes NHEJ in part by antagonizing end resection (Bouwman et al., 2010; Bunting et al., 2010). Strikingly, lentiviral constructs engineered to mutate the *53BP1* gene, but not off-target controls, reduced both the frequency and size of colonies formed in a Pol θ deficient background (Fig. 5B, Fig. S5). By comparison, there was no difference comparing targeting vs. non-targeting constructs in parallel experiments in wild type cells (Fig. S5). Our results thus identify a central role for TMEJ in repairing chromosome breaks when resection is excessive or mis-regulated.

We next sought to address whether defects in TMEJ might influence the efficiency of repair by HR of the same break studied in the experiments described above (Figs 4 and 5A). We generated breaks at the Cas9 site in chromosome 6 as above, but now included an extrachromosomal homology donor with 6 bp substituted at the target site that both ablates Cas9 recognition and introduces a site for the restriction endonuclease ScaI (Fig. 6A). Products of HR were thus scored as ScaI sensitive species in amplified products of the native chromosome flanking the Cas9 target; these were sensitive to depletion of Rad51 (Fig. S6A) and dependent on both the presence of the homology donor and the initiating DSB (Fig. 6B). We observed a frequency of HR in WT MEFs of 10%, and this is increased more than 2 fold in Ku70 deficient cells (Fig. 6C, S6B). By comparison, deficiency in Pol θ did not similarly result in increased HR. Indeed, loss of Pol θ in cells deficient in Ku70, where TMEJ otherwise accounts for a large fraction of repair, led instead to a slight decrease in HR efficiency. We note loss of Pol θ does increase a marker of an intermediate step in HR, ionizing radiation-induced Rad51 foci (Ceccaldi et al., 2015; Mateos-Gomez et al., 2015), but this effect was again less than that attributable to deficiency in Ku70 (Fig. S6C, S6D).

We conclude NHEJ effectively competes with HR for repair of nuclease-induced breaks (in accord with previous work) (Pierce et al., 2001), but that TMEJ does not.

Simultaneous breakage at two sites in the genome can lead to the joining of ends from different chromosomes, or translocation. We addressed the contribution of TMEJ to this process by again introducing breaks at the previously used Cas9 site in chromosome 6, but now also introduced a second break at a site in chromosome 11 (Fig. 6D). Genomic DNA was then harvested and used as template in emulsion PCRs (ddPCRs) to assess the frequency of the t(6;11) der11 translocation product. In accord with previous work (Weinstock et al., 2007), translocation frequency relative to WT cells was increased 3 fold in Ku70 deficient cells (Fig 6E). However, deficiency in Pol θ alone had no significant impact. Moreover, characterization of translocation products indicated that for each of the four cell types (WT, *Polq*$^{-/-}$, *Ku70*$^{-/-}$, and *Polq*$^{-/-}$*Ku70*$^{-/-}$), the frequency of junctions with microhomology was reduced relative to the products of intra-chromosomal deletion (Table S3). TMEJ thus does not promote formation of translocations under the conditions used here. More significantly, the frequency of translocation was highest when cells were deficient in both Pol θ and Ku70. TMEJ can thus protect against this class of chromosome rearrangement, though this effect was significant here only if cells are unable to efficiently repair breaks by NHEJ.

Discussion

Our results indicate that in cells, Pol θ has a central role in an end-joining pathway – TMEJ – that is uniquely able to repair substrates where classically defined NHEJ is ineffective (Fig. 2). The effects of Pol θ deficiency on both which substrates can be joined (Fig. 2) and product spectra (Figs. 3, 4) indicates that in mammals, Pol θ/TMEJ is required for most of what had previously been defined as MMEJ or Alt-NHEJ. Characterization of these products further argues TMEJ is an organized pathway, as synthesis by Pol θ is coupled to two prior steps, including a search for microhomology and removal of nonhomologous tails (Fig. 3). Moreover, we show deficiency in Pol θ alone has at best minor effects on activities of other pathways (NHEJ and HR) in the repair of a Cas9-induced break (Fig. 4, 6). TMEJ thus does not typically compete with these pathways. However, TMEJ has a critical role when there is excessive resection, i.e. cells deficient in Ku70 or 53BP1 (Fig. 1, 4, 5). We conclude Pol θ/TMEJ is essential for repair of DSBs when either major DSB repair pathway is compromised (Fig. 7), and both protects against or promotes genome instability dependent on context (Fig. 6 and discussed below).

Identification of biologically significant substrates and mechanism

We show there are marked differences between cellular TMEJ and the in vitro activities of the truncated Pol θ polymerase domain (Kent et al., 2015; Yousefzadeh et al., 2014). TMEJ is uniquely required as ssDNA extensions exceed 45 nt (Fig.2), as well as forked ends (i.e. when a paired 5′ terminus is unavailable); by comparison, *in vitro* studies (Kent et al., 2015) indicate activity was limited to extensions 15 nt or shorter. We suggest full length Pol θ may be intrinsically more processive (Arana et al., 2008), Pol θ may employ a processivity clamp (PCNA) during cellular TMEJ, or there may be polymerase switching after synthesis

initiation. The unique activity on forked structures is consistent with studies identifying an important role for Pol θ in replication fork re-start after fork collapse ("one-ended" chromosome breaks) (Ceccaldi et al., 2015; Roerink et al., 2014). Indeed, this result predicts TMEJ will be critical in joining any pair of ends where either of the 5′ termini is inaccessible to Ku or "unligatable", i.e. has irreversible bulky adducts or is associated with extensive base damage.

Cellular TMEJ is also rarely associated with synthesis from terminal mispairs (Fig. 3B), as can be observed in in vitro studies of truncated Pol θ activity (Kent et al., 2015). This limitation could dramatically restrict the fraction of ends that could be joined (<1/64), given the requirement for annealing at significant microhomologies (3-6 bp) for synthesis. Our results indicate cellular TMEJ instead efficiently samples all of the useable alignments within the 3′ terminal 25 nt of a pair of ends, which is sufficient to enable efficient joining of over 99% of ends of random sequence. The spectrum of cellular TMEJ products also emphasizes another advantage of a homology-search mechanism, its ability to mitigate deletion. 91% of TMEJ-dependent products of an extrachromosomal substrate with 140 nucleotides of ssDNA have less than 50 bp (2×25) of deletion. Consistent with this result, the effect of Pol θ deficiency on chromosomal repair is normally restricted to deletions ranging from 5-50 bp (Fig. 4B, 4C).

Cellular TMEJ is thus made flexible, and deletion constrained, through an ability to tightly couple together three steps (Fig. 7): 1) a microhomology search that usually generates nonhomologous tails, 2) excision of these tails, and 3) synthesis from the newly annealed 3′ terminus. The search for microhomology might be dependent on the Pol θ N-terminal helicase-like domain, as suggested by a structural model for an oligomer of this domain that juxtaposes a pair of 3′ssDNA termini (Newman et al., 2015). In accord with this model, the ability to use embedded alignments is specifically impaired in cells expressing a Pol θ mutation that inactivates this domain's ATPase activity. Effects of ATPase activity on microhomology search could plausibly be explained if it drove adjustment of the relative position of the two aligned termini. With regard to the next step, removal of nonhomologous 3′ tails, Pol θ has no intrinsic nuclease activity (Yousefzadeh and Wood, 2013). However, such an activity is present as a contaminant of Pol θ partially purified from HeLa cells (Maga et al., 2002), and results described here suggest this activity is tightly coupled to Pol θ activity. Mre11 and XPF-ERCC1 are both attractive candidates for this nuclease activity, as they have appropriate substrate specificities and have already been implicated in Alt-NHEJ/MMEJ (Bennardo et al., 2008). The third step, synthesis from 3′ termini with 3- 6 bp annealed, is facilitated by the tight grasp Pol θ maintains on the primer termini (Zahn et al., 2015). Altogether, Pol θ is uniquely suited to direct this pathway.

Role of TMEJ in double strand break repair

What is the relationship between previously defined Alt-NHEJ/MMEJ and Pol θ-dependent repair/TMEJ? Microhomology associated deletions typically used to define Alt-NHEJ/MMEJ are severely depleted in both Pol θ deficient contexts (i.e. *Polq*$^{-/-}$ and *Polq*$^{-/-}$*Ku70*$^{-/-}$), relative to their matched *Polq* proficient counterparts (Fig. 4). Similarly, Alt-NHEJ has been defined as dependent on prior resection of ends, and we determined the effect of Pol θ

deficiency on microhomology associated deletions is comparable to deficiency in a factor required for end resection, Mre11 (Fig. 5A). There is also little evidence for repair of pre-resected extrachromosomal substrates in cells deficient in both Pol θ and Ku70 (Fig. 2). Taken together, our evidence indicates TMEJ accounts for the majority of events previously defined as MMEJ or Alt-NHEJ. Nevertheless, chromosomal end-joining products still accumulate in *Polq*$^{-/-}$*Ku70*$^{-/-}$ cells (Fig. 4B). This may represent residual repair mediated by the remaining NHEJ components, or an as yet un-defined and largely microhomology-independent alternative to the end-joining pathways referenced so far (Alt-NHEJ/MMEJ/TMEJ and NHEJ).

In cells proficient in both NHEJ and HR, loss of Pol θ significantly affects only a small fraction (<5%) of DSB repair (Fig. 4C), consistent with mild phenotypes of cells and mice deficient in Pol θ alone (Shima et al., 2004). TMEJ is also associated only with deletions of intermediate size (5-50 bp) in this context. By comparison, TMEJ is engaged more rapidly, more often, and affects a wider range (5-250 bp) of deletions in cells deficient in Ku70/NHEJ. Cell growth and viability are also severely impaired in cells deficient in both Pol θ and Ku70 (Fig. 1), or Pol θ and 53BP1 (Fig. 5); the latter factor is more specifically associated with attenuation of end resection than is Ku70. Our results are thus consistent with a central role for TMEJ when end structures are poor substrates for NHEJ, as well as in cells prone to excessive end resection (Fig. 7).

Homology-dependent repair of Cas9-induced breaks was stimulated more than two fold by loss of Ku70. In contrast, loss of Pol θ had no significant effect on HR of the same break, even in a Ku70 deficient background. TMEJ is thus a less effective competitor than is NHEJ for repair of DSBs, at least when the DSBs are destined for successful repair. A similar lack of effect of Pol θ deficiency on repair by HR is evident in *C. elegans* (van Schendel et al., 2015). Pol θ loss is nevertheless sufficient to stimulate IR-dependent Rad51 foci (Ceccaldi et al., 2015; Mateos-Gomez et al., 2015) (Fig. S6C, S6D), which could reflect the accumulation of products of aborted HR that are no longer resolved by Pol θ-dependent means.

Previous work identified a key role for TMEJ in repair of chromosome breaks in homologous-recombination deficient cancer cell lines (Ceccaldi et al., 2015; Mateos-Gomez et al., 2015). Here we find the events we can attribute to Pol θ/TMEJ – deletions that are less than 50 bp and associated with flanking microhomologies >2 bp or insertions > 4 bp – is precisely equivalent to a mutational signature associated with those breast, ovarian, and pancreatic cancers that have mutations in BRCA1 and BRCA2 (COSMIC Signature 3) (Alexandrov et al., 2013).

Strikingly, 53BP1 loss has opposite effects on cell viability when comparing cells deficient in Pol θ vs. cells deficient in BRCA1; it impairs growth and viability in the former context (Fig. 5B), but rescues it in the latter (Bouwman et al., 2010; Bunting et al., 2010). Of special note is the ability of 53BP1 loss to “protect” BRCA1 deficient cancers from therapies that employ inhibitors of poly(ADP)ribose polymerase. Our data indicate Pol θ/TMEJ activity will be essential in the context of this mechanism of therapy resistance. These results

emphasize the critical importance of appropriately regulated end-resection, and further emphasizes the importance of Pol θ/TMEJ as a therapeutic target.

TMEJ and genome instability

There is evidence that Pol θ/TMEJ both suppresses and promotes DSB-induced chromosome rearrangement. Pol θ was identified in a systematic screen for suppressors of spontaneous genome instability (Shima et al., 2003), and it additionally suppresses translocations associated with immunoglobulin class switch recombination (Yousefzadeh et al., 2014). We report here that Pol θ can also suppress translocations between a pair of Cas9-induced breaks targeted to different chromosomes, though a significant effect was limited to cells already deficient in NHEJ (Fig. 6B). Moreover, the fraction of these translocation products associated with a TMEJ-like signature (e.g. microhomologies) was reduced relative to matched products of intra-chromosomal deletion for all four cell types.

In contrast, a previous report assessing Cas9-induced translocations indicated these were promoted by Pol θ, and Pol θ was required in NHEJ deficient cells for fusion of chromosomes at de-protected telomeres (Mateos-Gomez et al., 2015). Additionally, this and related studies (Simsek and Jasin, 2010) indicate translocation products are often enriched for TMEJ-associated signatures. Moreover, as also noted above, this signature is associated with deletions observed in hereditary breast cancer (Alexandrov et al., 2013).

Results described here also suggest how Pol θ/TMEJ could promote chromosome rearrangement. Analysis of intra-chromosomal deletions identified frequent “template-switching” events; these insertions were assembled from multiple template segments, sometimes from opposite strands, and often with 2-4 bp microhomologies associated with the flanks of successive segments. Importantly, promiscuity in template switching extended to surprisingly frequent switching to template tracts in other chromosomes (1.5×10^{-3} of total products in Ku70 deficient cells). We note our ability to recover examples of switching of template to another chromosome required a “switching back” of the repair process, such that the rejoined product remained intrachromosomal. It thus seems likely there is an undetected fraction of these events – perhaps even the majority – that never switch back, and contribute to chromosome aberrations similar to the microhomology-mediated break induced replication (MM-BIR) events described in yeast and mediated by Pol ζ and Rev1 (Sakofsky et al., 2015).

This varied contribution of Pol θ/TMEJ to genome instability in mammalian cells may reflect differences in the origin of the chromosome break and cell type. Notably, evidence that TMEJ suppresses genome instability comes from analysis of populations of primary cells, and where the assessed chromosome aberrations arise from chromosome breakage that was spontaneous (Shima et al., 2004) or naturally programmed (Yousefzadeh et al., 2014). The properly regulated use of TMEJ as a backup mechanism thus may protect against genome instability. However, as is apparent in hereditary breast cancer, defective DNA damage responses in transformed cell lines and cancers can result in excessive engagement of TMEJ and even an “addiction” to this pathway (Ceccaldi et al., 2015; Higgins et al., 2010; Lemée et al., 2010; Mateos-Gomez et al., 2015). The ability of Pol θ/TMEJ to promote genome instability may thus be acquired in parallel with the transition of its role

from backup to essential. In sum, this work identifies Pol θ as a critical factor in the survival and evolution of cancers deficient in canonical repair pathways, as well as a promising target for the treatment of these cancers.

Experimental Procedures

Detailed descriptions of the reagents (e.g. oligonucleotides, antibodies) are available in supplemental experimental procedures.

Accession numbers

Sequences generated in this study are available at NCBI SRA (Biosample SAMN05213772).

Cell lines

Experiments varying *Polq* status (excepting Fig. 1B) employed T antigen transformed MEFs recovered from mice (Yousefzadeh et al., 2014) where a Polq null allele was generated by conventional gene targeting and made isogenic by backcrossing in mice (Shima et al., 2004). *Polq-/-* MEFs were then complemented by cDNA expression (Yousefzadeh et al., 2014), with deficiency or complementation re-assessed to be concurrent with the experiments described here (Fig. S1A). Variants of the above lines with frameshift mutations in Exon 3 of the *Ku70* gene were made following transient expression of Cas9 and sgRNA, and complemented variants of these Ku70 deficient lines made with lentivirus expressing mouse Ku70. Ku70 deficiency or complementation was validated by western analysis (Fig. S1B) and a functional assay for NHEJ activity (Fig. S1C). In Figs. 1B and Fig. 5 experiments, the relevant genes were mutagenized with lentivirus that co-expressed Cas9 and sgRNA.

DSB Repair assays

For Figs. 1-3, 75 ng of 611bp linear fragments with end structures varied as noted and 1 ug pMAX-GFP (Lonza) were introduced into 2×10^5 cells by electroporation (Neon, Invitrogen) using a 1350 V, 30 ms pulse in a 10 μL chamber and incubated for 1 hour. Cells were washed, incubated with 12.5U of Benzonase (Sigma) to digest extracellular substrate, and cellular DNA purified (QIAamp DNA mini kit, Qiagen) to use as template for qPCR quantification of recovered product (Fig. 2, 3) and substrate (Fig. S2E) (supplemental experimental procedures) and sequencing.

For Figs. 4-6, plasmids expressing Cas9 (5 ug) and *Rosa26* sgRNA (5 ug) were introduced by electroporation as above except with 2×10^6 cells and a 100 uL chamber. These plasmids were supplemented with a homology donor (20ug) for Fig. 6B and 6C experiments, and a plasmid expressing *H3f3b* sgRNA (5 ug) for Fig. 6E experiments. Cas9 expression was assessed by western blot. Genomic DNA was harvested at noted times, purified (QIAamp DNA mini kit), and amplified products characterized by electrophoresis or sequencing. Recombination was measured by PCR amplification of the target site and digestion with ScaI. Dependency on Rad51 was confirmed by transfection of 20 nM control or Rad51 targeting siRNA pools prepared with RNAimax (Thermo). Depletion of Rad51 was confirmed by western blot. Translocation frequency was determined by ddPCR quantification of amplified translocation product, with a parallel ddPCR used to count input

genomes (supplemental experimental procedures). Parallel reactions were also chloroform extracted, and sequenced using standard methods.

Rosa26 repair product sequences (~50,000/each biological replicate) were obtained using Miseq 2 × 150 bp (Fig. 3) or 2 × 300 bp (Fig. 4) runs (Illumina). Each sample, as well as a control to validate proportional sampling of the initial population (supplemental experimental procedures), was amplified with barcoded primers and sequenced independently. Junctions were characterized in CLC Genomics Workbench 8 and Microsoft Excel. Insertions >24 bp (Fig. 4E, Table S2) were mapped against the reference mouse genome with batch BLAST searches.

S-phase cells and chromosomal aberrations

S-phase cells were quantified by flow cytometry after cells were treated with 10 uM BrdU (Sigma) for 1 hour, fixed, washed with PBS, treated with 0.1 M HCl/0.5% Triton X-100, and stained for both total DNA and incorporated BrdU.

Chromosomal aberrations (breaks, fragments, and fusions) were counted after cells were treated with 50 ng/ml colcemid for 45 min, lysed, fixed, and stained with Giemsa (Gibco).

Gel Shift

5 nM Cy-5 labeled DNA substrates were incubated with 500 nM Streptavidin for 10 minutes, then incubated with 5nM Ku for 5 minutes at 37°C be fore addition of a 10-fold excess of unlabeled dsDNA and electrophoresis.

Immunofluorescence

Cells were irradiated with 1 Gy of gamma radiation and incubated for 6 hours, then washed, fixed, permeabilized, and stained to detect nuclear material (DAPI) and Rad51 foci (supplemental experimental procedures).

Supplementary Material

Refer to Web version on PubMed Central for supplementary material.

Acknowledgments

Our studies were supported by NCI grant CA097096 (D.A.R), AHA grant 14PRE20380258 (D.W.W), RP130297 and RP150102 from the Cancer Prevention and Research Institute of Texas and the Grady F. Saunders Research Professorship (R.D.W.), T32 CA09480 (MJY), DOD grant BC141727 and NIEHS grant R00ES02633 (S.A.R.), and the Burroughs Welcome Fund Career Award for Medical Scientists (G.P.G.). We thank Luis Blanco for the gift of *Polm*$^{-/-}$*Pol*$^{-/-}$ MEFs and Juan Carvajal-Garcia and George W. Small for methods development.

References

Alexandrov LB, Nik-Zainal S, Wedge DC, Aparicio SAJR, Behjati S, Biankin AV, Bignell GR, Bolli N, Borg A, Børresen-Dale AL, et al. Signatures of mutational processes in human cancer. Nature. 2013; 500:415–421. [PubMed: 23945592]

Aparicio T, Baer R, Gautier J. DNA double-strand break repair pathway choice and cancer. DNA Repair (Amst). 2014; 19:169–175. [PubMed: 24746645]

Arana ME, Seki M, Wood RD, Rogozin IB, Kunkel TA. Low-fidelity DNA synthesis by human DNA polymerase theta. Nucleic Acids Res. 2008; 36:3847–3856. [PubMed: 18503084]

Bennardo N, Cheng A, Huang N, Stark JM. Alternative-NHEJ is a mechanistically distinct pathway of mammalian chromosome break repair. PLoS Genetics. 2008; 4:e1000110. [PubMed: 18584027]

Boulton SJ, Jackson SP. Saccharomyces cerevisiae Ku70 potentiates illegitimate DNA double-strand break repair and serves as a barrier to error-prone DNA repair pathways. The EMBO Journal. 1996

Bouwman P, Aly A, Escandell JM, Pieterse M, Bartkova J, van der Gulden H, Hiddingh S, Thanasoula M, Kulkarni A, Yang Q, et al. 53BP1 loss rescues BRCA1 deficiency and is associated with triple-negative and BRCA-mutated breast cancers. Nat Struct Mol Biol. 2010; 17:688–695. [PubMed: 20453858]

Bunting SF, Callén E, Wong N, Chen HT, Polato F, Gunn A, Bothmer A, Feldhahn N, Fernandez-Capetillo O, Cao L, et al. 53BP1 inhibits homologous recombination in Brca1-deficient cells by blocking resection of DNA breaks. Cell. 2010; 141:243–254. [PubMed: 20362325]

Ceccaldi R, Liu JC, Amunugama R, Hajdu I, Primack B, Petalcorin MIR, O'Connor KW, Konstantinopoulos PA, Elledge SJ, Boulton SJ, et al. Homologous-recombination-deficient tumours are dependent on Polθ-mediated repair. Nature. 2015; 518:258–262. [PubMed: 25642963]

Chan SH, Yu AM, McVey M. Dual roles for DNA polymerase theta in alternative end-joining repair of double-strand breaks in Drosophila. PLoS Genetics. 2010; 6:e1001005. [PubMed: 20617203]

Higgins GS, Harris AL, Prevo R, Helleday T, McKenna WG, Buffa FM. Overexpression of POLQ confers a poor prognosis in early breast cancer patients. Oncotarget. 2010; 1:175–184. [PubMed: 20700469]

Kabotyanski EB, Gomelsky L, Han JO, Stamato TD, Roth DB. Double-strand break repair in Ku86- and XRCC4-deficient cells. Nucleic Acids Res. 1998; 26:5333–5342. [PubMed: 9826756]

Kent T, Chandramouly G, McDevitt SM, Ozdemir AY, Pomerantz RT. Mechanism of microhomology-mediated end-joining promoted by human DNA polymerase θ. Nat Struct Mol Biol. 2015; 22:230–237. [PubMed: 25643323]

Lee K, Lee SE. Saccharomyces cerevisiae Sae2- and Tel1-dependent single-strand DNA formation at DNA break promotes microhomology-mediated end joining. Genetics. 2007; 176:2003–2014. [PubMed: 17565964]

Lemée F, Bergoglio V, Fernandez-Vidal A, Machado-Silva A, Pillaire MJ, Bieth A, Gentil C, Baker L, Martin AL, Leduc C, et al. DNA polymerase theta up-regulation is associated with poor survival in breast cancer, perturbs DNA replication, and promotes genetic instability. Proceedings of the National Academy of Sciences of the United States of America. 2010; 107:13390–13395. [PubMed: 20624954]

Maga G, Shevelev I, Ramadan K, Spadari S, Hübscher U. DNA polymerase theta purified from human cells is a high-fidelity enzyme. Journal of Molecular Biology. 2002; 319:359–369. [PubMed: 12051913]

Mateos-Gomez PA, Gong F, Nair N, Miller KM, Lazzerini-Denchi E, Sfeir A. Mammalian polymerase θ promotes alternative NHEJ and suppresses recombination. Nature. 2015; 518:254–257. [PubMed: 25642960]

Newman JA, Cooper CDO, Aitkenhead H, Gileadi O. Structure of the Helicase Domain of DNA Polymerase Theta Reveals a Possible Role in the Microhomology-Mediated End-Joining Pathway. Structure. 2015; 23:2319–2330. [PubMed: 26636256]

Pierce AJ, Hu P, Han M, Ellis N, Jasin M. Ku DNA end-binding protein modulates homologous repair of double-strand breaks in mammalian cells. Genes Dev. 2001; 15:3237–3242. [PubMed: 11751629]

Pryor JM, Waters CA, Aza A, Asagoshi K, Strom C, Mieczkowski PA, Blanco L, Ramsden DA. Essential role for polymerase specialization in cellular nonhomologous end joining. Proceedings of the National Academy of Sciences of the United States of America. 2015; 112:E4537–E4545. [PubMed: 26240371]

Roerink SF, van Schendel R, Tijsterman M. Polymerase theta-mediated end joining of replication-associated DNA breaks in C. elegans. Genome Res. 2014; 24:954–962. [PubMed: 24614976]

Sakofsky CJ, Ayyar S, Deem AK, Chung WH, Ira G, Malkova A. Translesion Polymerases Drive Microhomology-Mediated Break-Induced Replication Leading to Complex Chromosomal Rearrangements. Mol Cell. 2015; 60:860–872. [PubMed: 26669261]

Sfeir A, Symington LS. Microhomology-Mediated End Joining: A Back-up Survival Mechanism or Dedicated Pathway? Trends in Biochemical Sciences. 2015; 40:701–714. [PubMed: 26439531]

Shima N, Munroe RJ, Schimenti JC. The mouse genomic instability mutation chaos1 is an allele of Polq that exhibits genetic interaction with Atm. Mol Cell Biol. 2004; 24:10381–10389. [PubMed: 15542845]

Shima N, Hartford SA, Duffy T, Wilson LA, Schimenti KJ, Schimenti JC. Phenotype-based identification of mouse chromosome instability mutants. Genetics. 2003; 163:1031–1040. [PubMed: 12663541]

Simsek D, Jasin M. Alternative end-joining is suppressed by the canonical NHEJ component Xrcc4-ligase IV during chromosomal translocation formation. Nat Struct Mol Biol. 2010; 17:410–416. [PubMed: 20208544]

van Schendel R, Roerink SF, Portegijs V, van den Heuvel S, Tijsterman M. Polymerase Θ is a key driver of genome evolution and of CRISPR/Cas9-mediated mutagenesis. Nat Commun. 2015; 6:7394. [PubMed: 26077599]

Weinstock DM, Brunet E, Jasin M. Formation of NHEJ-derived reciprocal chromosomal translocations does not require Ku70. Nat Cell Biol. 2007; 9:978–981. [PubMed: 17643113]

Yousefzadeh MJ, Wood RD. DNA polymerase POLQ and cellular defense against DNA damage. DNA Repair (Amst). 2013; 12:1–9. [PubMed: 23219161]

Yousefzadeh MJ, Wyatt DW, Takata KI, Mu Y, Hensley SC, Tomida J, Bylund GO, Doublié S, Johansson E, Ramsden DA, et al. Mechanism of suppression of chromosomal instability by DNA polymerase POLQ. PLoS Genetics. 2014; 10:e1004654. [PubMed: 25275444]

Zahn KE, Averill AM, Aller P, Wood RD, Doublié S. Human DNA polymerase θ grasps the primer terminus to mediate DNA repair. Nat Struct Mol Biol. 2015; 22:304–311. [PubMed: 25775267]

Highlights

- Pol θ directs end-joining by coupling a microhomology search to synthesis across ends
- Pol θ mediated end-joining is critical when either canonical repair pathway fails
- Pol θ is also essential when cells aberrantly regulate resection of chromosome breaks
- Pol θ-dependent repair can both suppress and promote genome instability

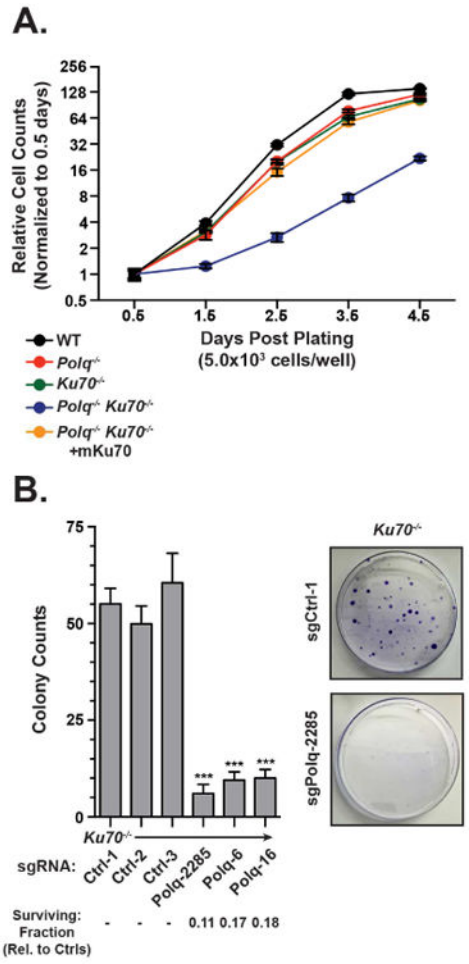

Figure 1. Effect of end-joining deficiencies on cell proliferation

(A) The noted cell types were seeded at 5×10^3 cells/well in 24 well dishes, then counted 12 hours after plating and every 24 hours afterwards. Data shown are the mean +/- SEM, n=3. **(B)** *Ku70*$^{-/-}$ cells were infected with lentivirus containing Cas9 and either control guides or guides targeting sites in regions coding for mouse Pol θ, seeded into 10 cm plates, and stained after 10 days (right panel). Colonies of more than 100 cells were counted from triplicate experiments (left panel); Data shown are the mean +/- SEM, n=3. Statistical significance was assessed by ANOVA with Bonferoni correction for multiple comparisons. ***p<0.001. See also Figure S1.

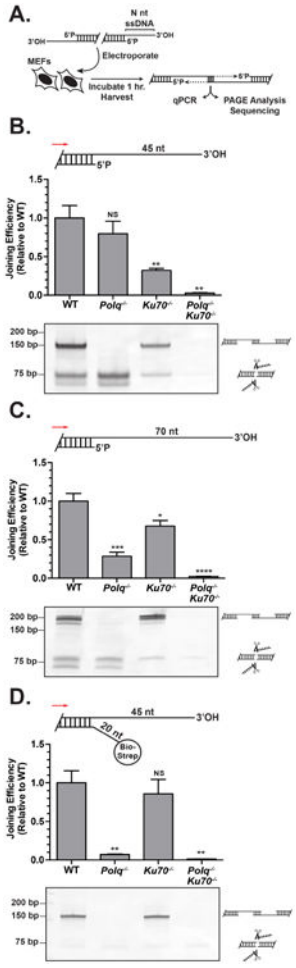

Figure 2. Effect of end-joining deficiencies on repair of pre-resected ends

(A) Linear substrates with varied end structures were introduced into noted cell types and end-joining products characterized by quantitative polymerase chain reaction (top panels) or electrophoresis of amplified products (bottom panels); Data shown below are the mean +/- SEM, n=3. Statistical significance was assessed by one-way ANOVA with Bonferoni correction of *p* values to account for multiple comparisons. NS not significant, **p*<0.05, ***p*<0.01, ****p*<0.001, *****p*<0.0001.

(B) A substrate with symmetrical 45 nt 3′ single stranded DNA overhangs was introduced into the noted cell types, and the mean efficiency of end-joining determined by qPCR and expressed as a fraction of that observed in WT cells. Amplified products generated in a parallel fixed-cycle number PCR were also characterized by electrophoresis; products of size consistent with joining after overhang clipping vs. overhang retention are noted.

(C) A substrate with 70 nt 3′ overhangs was introduced into the noted cell lines and joining characterized as described above.

(D) A substrate as in panel B, except with a 20 nt non homologous tail ending in a 5′ terminal biotin-streptavidin group, was introduced into the noted cell lines and joining characterized as described above. See also Figure S2.

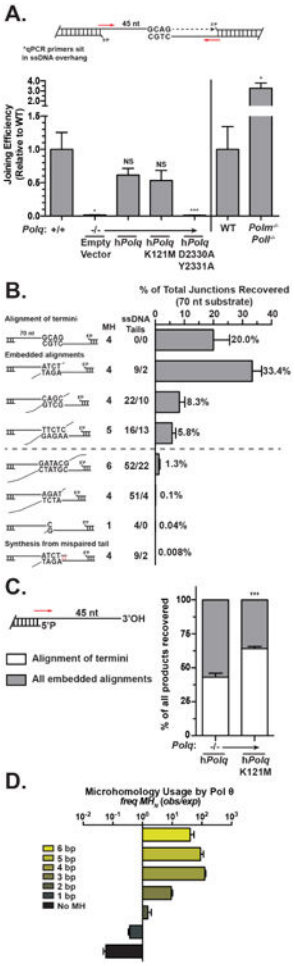

Figure 3. Mechanism of Pol θ mediated end-joining

(A) The 45 nt 3′ overhang substrate described in Fig. 2B was introduced into cells that were WT, *Polq*$^{-/-}$, and *Polq*$^{-/-}$ engineered to express wild type human *Polq* or variants deficient in helicase-like domain ATPase activity (K121M), or polymerase activity (D2330A+Y2331A), and joining efficiency assessed by qPCR using primers that require retention of at least 10 nt of each 3′ overhang sequence in junctions. Joining efficiency was also characterized in *Poll*$^{-/-}$*Polm*$^{-/-}$ MEFs, relative to matched WT control MEFs. Data shown are the mean +/- SEM, n=3. Statistical significance was assessed by one-way ANOVA with Bonferoni correction. NS =not significant, *p<0.05, **p<0.01, ***p<0.001.

(B) Observed frequency of different joining products of the 70 nt overhang substrate (Fig. 2C) recovered from wild type cells, including the 4 most common products (above dashed line) and 4 other representative examples (see also Table S1). The first 3 columns summarize the structures of the inferred intermediates.

(C) For experiments described in Fig. 3A (using the 45 nt overhang) we report the fraction of products directed by the terminal 4 bp microhomology (shown in panel B), as determined by sequencing. Data shown are the mean +/- SEM, n=3. Statistical significance was assessed by two-way ANOVA (p values as above).

(D) The extent each sized microhomology is enriched (bars right of Y axis) or depleted (bars left of Y axis) in recovered junctions, relative to their representation in the set of all possible deletion products. See also Figure S3, Table S1.

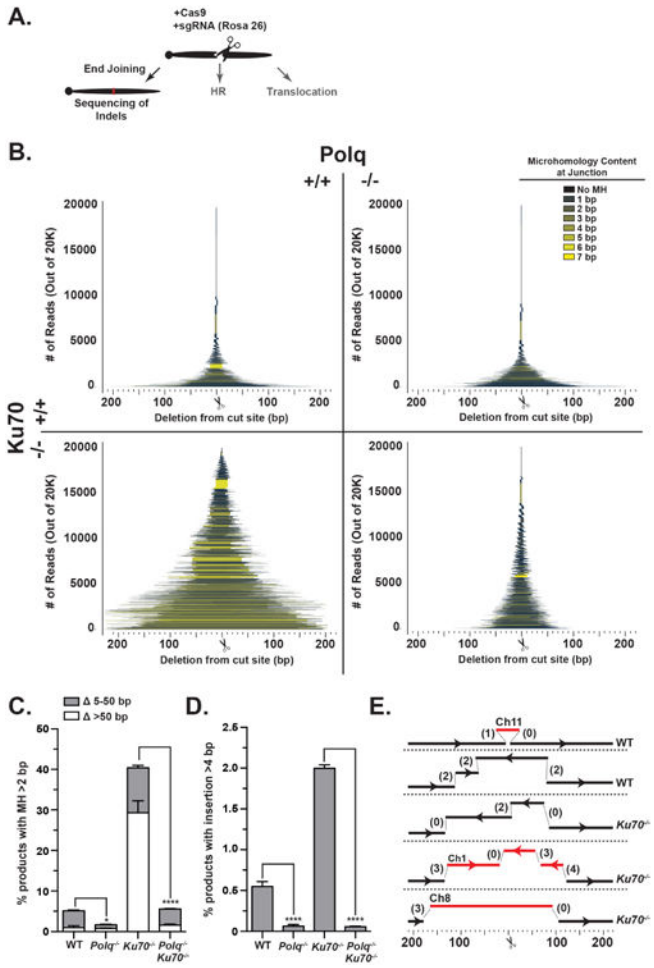

Figure 4. Effect of end-joining deficiencies on repair of Cas9-induced chromosome breaks

(A) Cas9 and guide RNA specific to a chromosome 6 target were expressed in the noted cell types, and products of end-joining characterized by target site amplification and sequencing.

(B) Bars denote extent of deleted DNA for each end-joining product relative to the Cas9 target site, and are shaded according to the extent of microhomology as noted in the legend. The height of each bar on the Y axis defines the proportion of each product in a set of 20,000 estimated input molecules, and is averaged from 3 experiments for each of WT (top left), *Polq*$^{-/-}$(top right), *Ku70*$^{-/-}$, (bottom left), and *Polq*$^{-/-}$*Ku70*$^{-/-}$ cells (bottom right).

(C) The percentage of all end-joining products with microhomology >2 bp and deletion (Δ) within the noted size ranges. Data shown are the mean +/- SEM, n=3. Statistical significance was assessed by two-way ANOVA with Bonferoni correction (results for the 5-50 bp category shown). *p<0.05, ****p<0.0001.

(D) The percentage of all end-joining products with insertion >4 bp recovered from MEF lines described above. Data shown are the mean +/- SEM, n=3. Statistical significance was assessed by one-way ANOVA with Bonferoni correction (p values as above).

(E) Structure of selected Pol θ mediated insertions. Successive segments denote template switching, with opposing arrows identifying use of opposite strands. The lengths of

microhomologies in flanks of successive segments are in parentheses. Black segments, from chromosome 6; red segments, from other chromosomes. See also Figure S4, Table S2.

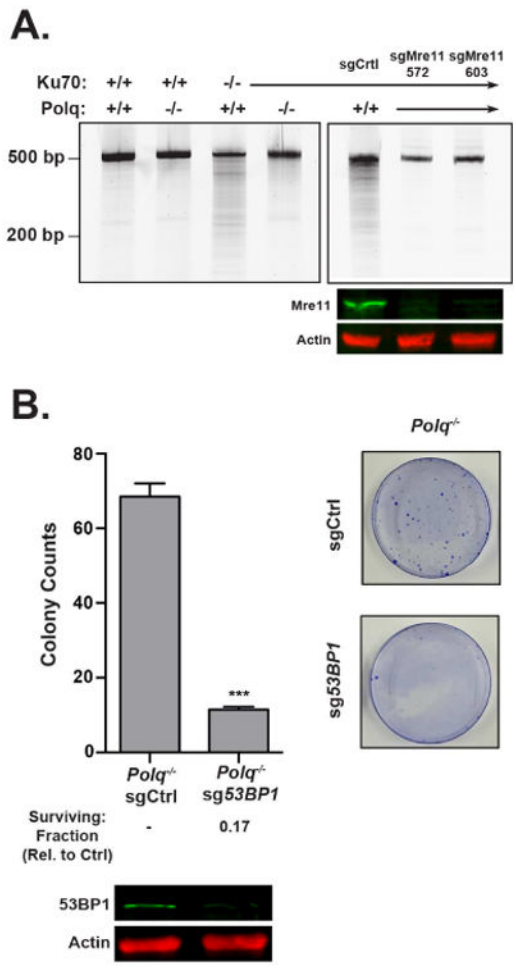

Figure 5. Effect of aberrant end resection on repair and viability

(A) Template DNA from the experiment described in Fig. 4 (left panel), or from *Ku70*$^{-/-}$ cells infected with lentivirus containing Cas9 and either a pool of control guides or guides targeting Mre11 at amino acids 572 or 603 respectively (right panel), was amplified and characterized by electrophoresis.

(B) *Polq*$^{-/-}$ cells were infected with lentivirus containing Cas9 and a pool of either control guides or guides targeting *53BP1*. Colony forming ability was assessed as in Fig. 1B. Data shown are the mean +/- SEM, n=3. Statistical significance was assessed by unpaired T-test. ***p<0.001. See also Figure S5.

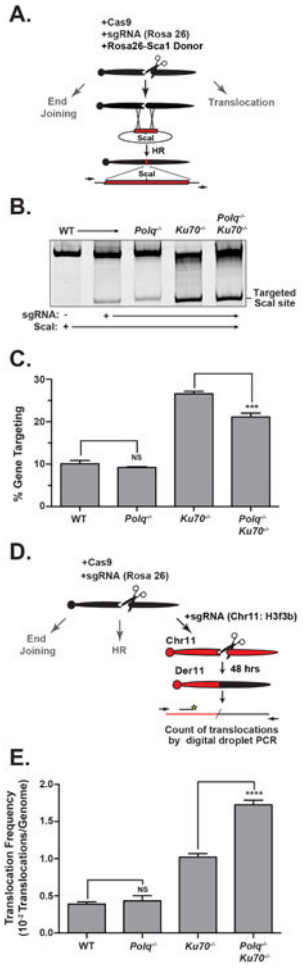

Figure 6. Effect of end-joining deficiencies on repair of chromosomal breaks by homologous recombination and translocation

(A, B) Homologous recombination was assessed by introduction of Cas9, guide RNA, and a plasmid homology donor that introduces a ScaI recognition site at the site of breakage in chromosome 6 into noted cell types. DNA was harvested 48 hours later, amplified, and digested with ScaI followed by electrophoresis.

(C) The mean fraction of the chromosome 6 target site that acquired sensitivity to ScaI. Data shown are the mean +/- SEM, n=3. Statistical significance assessed by one-way ANOVA with Bonferoni correction. NS =not significant, ***p<0.001, ****p<0.0001.

(D) Cas9 and guide RNAs targeting chromosome 6 and chromosome 11 were expressed in the noted cell types. Genomic DNA was isolated after 48 hours and used as template for parallel emulsion PCRs (ddPCR) specific for the t(6,11) der11 translocation product and an input genome control.

(E) Mean frequency of der11 translocations is determined by the number of translocations over the number of input genomes; Data shown are the mean +/- SEM, n=3, with >4×10^4 genomes assessed/experiment. Statistical significance was assessed by one-way ANOVA with Bonferoni correction (p values as above). See also Figure S6, Table S3.

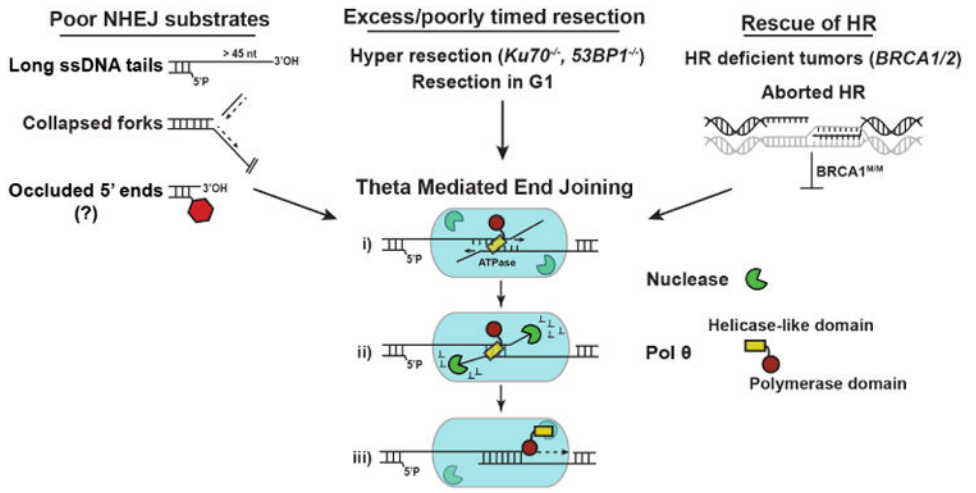

Figure 7. Mechanism and role of Pol θ mediated end-joining

Suggested contexts for engagement of Pol θ mediated end-joining, and proposed mechanism including a i) search for microhomology, ii) removal of non-homologous tails, and iii) synthesis.